

## Studies of Multiphase Flow in High Pressure Horizontal and +5 Degree Inclined Pipelines

Robert Wilkens and W. Paul Jepson  
 Ohio University  
 Athens, Ohio, USA

### ABSTRACT

In the process of oil production from older wells, brine and carbon dioxide gas are commonly present in the pipelines. Often these oil, water, and gas mixtures create a highly corrosive slug flow environment for typical carbon steel pipelines. The first step in understanding the enhanced corrosion is to characterize the nature of the flow. For this purpose, an 18-m long, 9.7-cm diameter, inclinable 316 stainless steel pipeline has been commissioned for the study of multiphase flow and its subsequent effects upon corrosion. Three component oil/water/gas mixtures with water cuts of 80 and 100% have been examined. At a temperature of 40 °C, flow patterns and slug characteristics were determined at inclinations of zero and five degrees, superficial liquid velocities of 0.1 to 1.5 m/s, superficial gas velocities of 1.0 to 11 m/s and system pressures of 0.27, 0.45, 0.79, and 1.13 MPa. A non-visual method, using measurement of differential pressure, was established to measure slug frequencies and determine flow patterns.

At an inclination of plus five degrees, the frequency of slugs was greater at the entrance to the test loop than further downstream at the test section. Additionally, the slug flow regime occurred at a lower superficial liquid velocity than in horizontal flow. No slugs were present in the downhill return for the matrix studied. The pressure drop increased with increasing gas and liquid flow rates, while decreasing slightly with an increase in pressure. The flow regime transitions for plug flow, slug flow, annular, and stratified flow were identified. Pressure had no apparent effect upon the plug flow/slug flow transition. However, as the pressure was increased, the slug flow regime became dominated by pseudo-slug flow. Slug frequency was observed to increase with increasing superficial gas and liquid velocities while varying little with pressure.

**KEYWORDS:** flow pattern, high-pressure, inclined flow, multiphase, non-visual, pressure drop, slug frequency

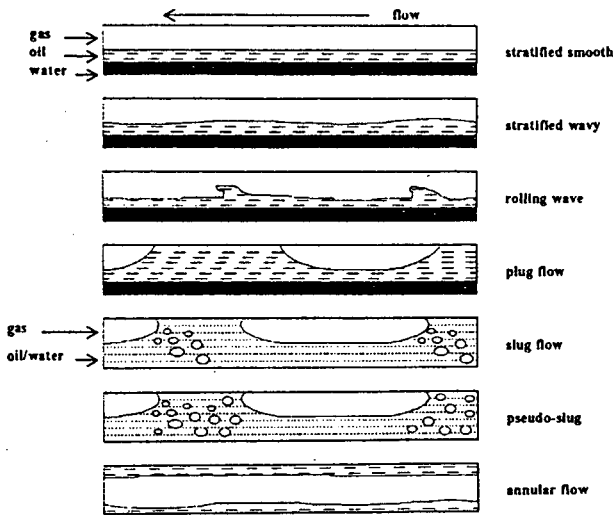
### INTRODUCTION

In the process of oil production from older wells, brine and carbon dioxide gas are commonly present in the pipelines. These oil, water, and gas mixtures can create a highly corrosive environment for typical carbon steel pipelines. To compound the problem, the oil wells are often at remote

locations forcing this corrosive mixture to be transported many miles before it can be separated. During this transport, the multiphase mixture travels through numerous changes of inclination which affects the flow pattern and flow characteristics. This can further enhance the corrosion.

The consequences of a major oil line break are undesirable. It is important to quantify the corrosivity of multiphase flow, under varying conditions, so effective corrosion control can be achieved. Corrosion inhibitors work by either adsorbing to the metal pipe surfaces or by reacting with corrosion products to form a protective layer. These inhibitors are added in either a batch or continuous process. Currently, corrosion inhibitors are not working well for slug flow conditions, Kaul (1995). The first step in determining the predominant corrosion mechanisms is to understand the nature of the flow.

Many researchers have attempted to produce multiphase flow pattern maps based on experimental data. Mandhane, *et al.*, (1974) created a two-phase map for horizontal, small-diameter, low-pressure flow using the superficial gas velocity,  $V_{sg}$ , and the superficial liquid velocity,  $V_{sl}$ , as parameters. This procedure has since become a standard in the oil industry. Taitel and Dukler (1976) proposed a mechanistic model for predicting flow patterns in two-phase gas-liquid flow. The basis for this model is the establishment of physical criteria for the transitions between five flow regimes. This model has been verified (Barnea, *et al.*, 1979) for small-diameter, low-pressure, two-phase systems at horizontal to near horizontal pipe flow. Jepson and Taylor (1993) demonstrated that the transitions did not hold for large-diameter pipes. Additionally, Lee (1993) demonstrated that the introduction of a third phase (a second, but immiscible, liquid) seriously affects the applicability of the Taitel and Dukler model. Figure 1 illustrates the typical flow patterns observed in oil/water/gas flow. At low liquid and gas flow rates, the three phases flow in a smooth stratified pattern. As the gas flow rate is increased, the interface between the oil and gas becomes wavy. If the liquid flows are increased, plug flow is reached. In three-phase plug flow, the oil/water interface remains stratified while intermittent gas pockets remove the oil from the top of the pipe. If the gas flow rate is increased from plug flow, the slug flow regime is reached. Characteristics of this slug flow include mixing of the oil and water layers, gas pockets of increased length, and gas bubble entrainment in the front of the slug, commonly referred to as the mixing zone. An additional increase in the gas velocity creates a flow pattern sometimes termed pseudo-slug flow. Pseudo-slugs have the same characteristics as slugs, but the mixing zone extends through the slug length allowing occasional gas blow-through to occur. At even higher gas flow rates, annular flow is reached. Annular flow exists when the less dense fluid (the gas) flows in a core along the center of the pipe while the more dense



fluid (the oil/water mixture) flows as an annular ring around the pipe wall.

Limited flow map data exists for inclined pipelines. Gould, *et al.*, (1974) introduced +45° and +90° flow pattern maps. Govier, *et al.*, (1972) presented a commonly used method of establishing flow patterns for inclined flow. Barnea, *et al.*, (1985) proposed a model for predicting transitions in inclined pipelines. Stanislav, *et al.*, (1986) reported inclined flow pattern data in small-diameter pipes as compared with a modified Taitel and Dukler model. Kokal and Stanislav (1986) characterized, extensively, the up-flow and down-flow patterns. However, all of these studies involved two-phase flow. Additionally, flow in large-diameter pipes and at high-pressure have not been studied.

In a detailed analysis of slug characteristics, Jepson (1989) suggests a breaking dam analogy in determining slug velocity. This is then used to show that the slug velocity increases with increasing gas flow rate. Gregory and Scott (1969) and Nicholson, *et al.*, (1978) reported slug frequency data and Nicholson, *et al.*, (1978) included data on pressure gradient and slug velocity. Jepson and Taylor (1993) also presented data for slug frequency, slug length, and pressure gradient as functions of superficial gas velocities. This data, however, is presented for two-phase, low-pressure flow in small-diameter, horizontal pipes. It does illustrate the clear interrelationship of these properties.

Due to the lack of available data, an 18-m long, 9.7-cm diameter, inclinable 316 stainless steel pipeline has been commissioned for the study of multiphase flow and its subsequent effects upon corrosion. This work studies the effects of three-phase (gas/liquid/liquid) flow in a large diameter pipe, including the effects of inclination and increasing pressure. Additionally, a non-visual method of flow pattern recognition has been established.

### NON-VISUAL FLOW DETERMINATION

Due to the high pressure requirement of the system, it was manufactured from 316 stainless steel. Thus, a non-visual method of flow pattern and property measurement had to be established and validated. Lin and Hanratty (1987) demonstrated that slugs could be detected, and their frequencies determined, by measuring single point pressure fluctuations. Additionally, they found that cross-correlating with another single point pressure, at a fixed distance from the first, allows for the determination of slug velocity. Spedding and Spence (1993) identified waves and films visually and reported the pressure fluctuations. These fluctuations, although not noted by the authors, appear to have characteristic shapes and magnitudes. The method of Lin and Hanratty (1987) could not be utilized for the high pressure system. A single point transducer with the proper range (on the order of megapascals) and with the proper sensitivity (on the order of a hundred pascals) would not be practical. Fan, Ruder, and Hanratty (1993)

demonstrated that as a slug passes a point on the pipeline wall, the pressure increases suddenly, continues to rise into the slug body, and rises further into the gas pocket forcing the slug down the pipe. From this, a technique was established for determining slug properties and flow patterns using differential pressure measurements.

In order to offset hydrostatic head differences in inclined flow, the high port of the transducer is placed downstream and the low port upstream. Thus, as the slug front reaches the first port, the differential pressure becomes negative. These differential pressure traces were first validated by direct comparison with visual observations in acrylic pipe. At a low pressure, differential-pressure traces between two ports 149 cm apart were coordinated with videotape for typical flow patterns in an oil/water/gas system with a 45% water cut. The videotape was analyzed frame-wise to obtain velocities, frequencies, and flow patterns. This was then compared to the differential pressure measurements. The flow patterns that were analyzed included stratified, full pipe, plug flow, slug flow, and slug-annular flow. Sample differential pressure traces for these flow types are given in Figures 2 - 6, respectively.

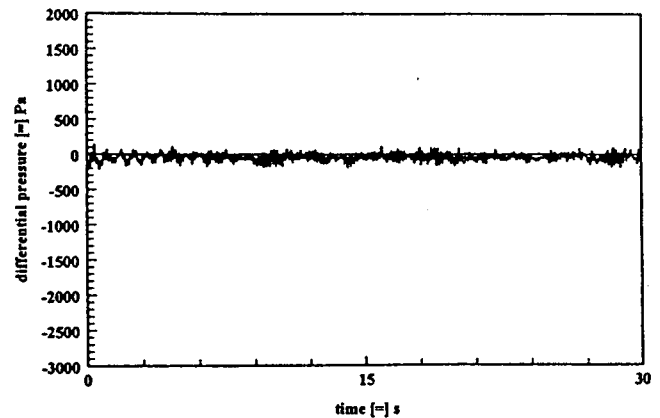


Figure 2: Stratified wavy flow sample differential pressure trace at low pressure.

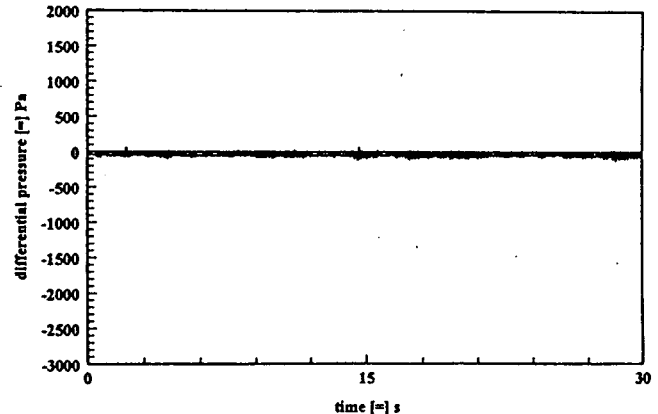


Figure 3: Full pipe flow sample differential pressure trace at low pressure.

Figures 2 and 3 demonstrate that stratified and full pipe flow show little fluctuation in differential pressure,  $\pm 100$  Pa. The plug flow differential pressure trace, Figure 4, appears as a low frequency sine wave with an amplitude of approximately 500 Pa and a few high frequency fluctuations. The plug flow trace shows approximately 12 plugs per minute. An analysis of the same flow conditions in a one minute videotape sequence indicated 14 plugs.

As slugs pass the test section, the differential pressure typically dips at least 1,500 Pa. Using this as a criterion, for the differential pressure trace in Figure 5, indicates slug flow with a frequency of approximately 16 slugs per minute. Reviewing the videotape of this flow also revealed slug flow with a slug frequency of 16 per minute. Additionally, the flow was observed to also have 14 rolling waves greater than half-pipe yet not large enough to

thermocouple connected to an electronic analyzer with display. The differential pressure is measured with two 0 - 35 kPa heavy duty differential pressure transducers at tap distances of 10 and 132 cm. The smaller distance was selected such that it responds as a mark in time and does not allow multiple slugs within its length. The transducers produce a current signal of 4 to 20 mA which is sent through a second-order low-pass filter, to eliminate frequencies greater than 10 kHz, and shunted with a 500-ohm resistor, across a data acquisition board giving a signal of 2 to 10 volts. A Pentium PC has been programmed to average 100 samples before reporting the value. This occurs at a rate of 60 values for each channel per second for an overall sampling rate of 12 kHz. Additional measurements are made using two multiphase acoustic sensors, placed 142 cm apart in the test section, with output sent to a digital oscilloscope.

Upon leaving the test section, the multiphase flow passes through a separator, to prevent siphoning due to the declined angle of flow return, and back into the mixing tank. The gas passes through a de-entrainment plate, through a separator and back-pressure regulator where it is then vented to the atmosphere.

The oil used in this study was a light oil petroleum distillate with a 2.0 cP viscosity and 800 kg/m<sup>3</sup> density. The water was ASTM seawater. All gas used was carbon dioxide. The system temperature was 40 °C. The matrix studied is listed in Table 1. Water cut is defined as the volume percent of the liquid which is occupied by water.

## RESULTS AND DISCUSSION

Tables 2 - 8 present pressure drop and slug frequency data for 100% water cut at 0° inclination and system pressures of 0.45 and 0.79 MPa. For each flow condition the velocity of the slug front,  $V_s$ , was 1.2 times the mixture velocity. With this information, three frequencies were determined:  $F_{S1}$ , the frequency at which the differential pressure change exceeded 1,500 Pa between the 132-cm taps;  $F_{S2}$ , the frequency at which the differential pressure change exceeded 150 Pa between the 10-cm taps;  $F_V$ , the frequency at which cross-correlation of the two traces revealed the appropriate time separation for a velocity of  $V_s$ , the translational velocity of the slug. Figures 9 and 10 are from the same differential pressure trace at different times. Figure 9 shows an example of a differential pressure fluctuation from a slug on an expanded time axis. The two parallel lines drawn are at a distance

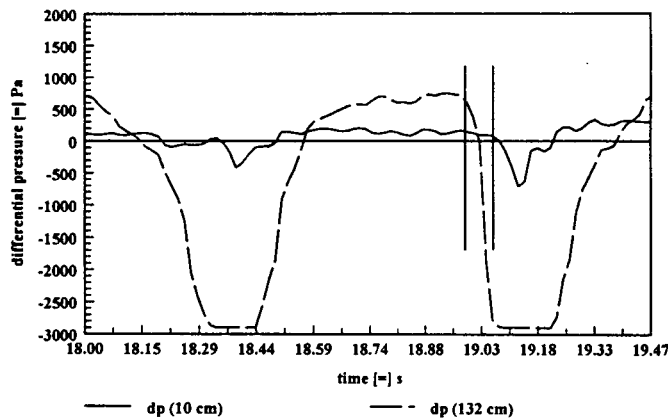


Figure 9: Slug differential pressure trace for  $V_{sl} = 1.0$  m/s,  $V_{sg} = 9.3$  m/s, 0.45 MPa.

0.074 seconds apart, corresponding to a velocity of  $V_s$  between the two taps. These lines were moved along the time axis to find where the fluctuations were consistent with this slug velocity. Figure 10 demonstrates that total pressure fluctuation alone does not indicate slug passage. An apparent slug reached the first set of taps at approximately 23 seconds. If this fluctuation represented a slug, it would reach the second set of taps approximately 0.074 seconds later. However, it does not reach the second set of taps until approximately 0.14 seconds later. This represents a velocity of only 50%  $V_s$ . It is proposed that  $F_V$  is the true slug frequency. Test section pressure drop was determined by the average difference of maxima and minima between leading and trailing films.

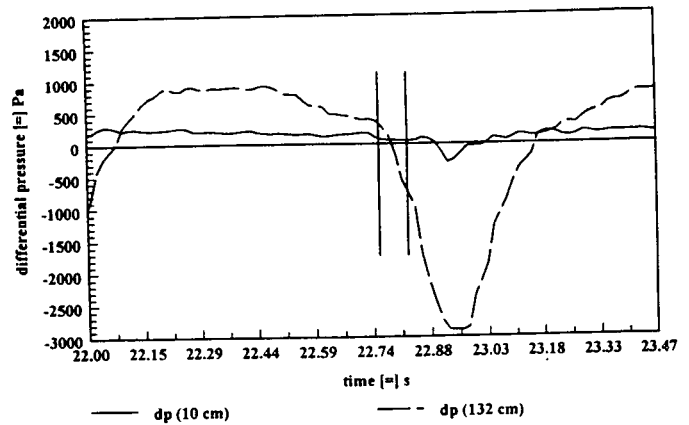


Figure 10: Slug differential pressure trace for  $V_{sl} = 1.0$  m/s,  $V_{sg} = 9.3$  m/s, 0.45 MPa.

$F_{S1}$  increased with increasing gas flow rates at the high liquid flow rates, while varying more erratically at the lower liquid flow rates. Table 3 shows that at a high superficial liquid velocity, 1.5 m/s,  $F_{S1}$  increased from 50 to 110 pulses per minute as the superficial gas velocity was increased from 1.7 to 10.3 m/s. Table 6 shows that at a low superficial liquid velocity, 0.5 m/s,  $F_{S1}$  varies at 14, 14, 6, 12, and 20 pulses per minute as the superficial gas velocity was set to 1.3, 3.3, 5.6, 7.6, and 8.3 m/s, respectively.

$F_{S1}$  also increased with increasing liquid flow rate. At a superficial gas velocity of approximately 3.4 m/s, Tables 3, 5, and 7 show that  $F_{S1}$  increased from 18 to 24 to 50 pulses per minute at superficial liquid velocities of 0.5, 1.0, and 1.5 m/s, respectively.

In the slug flow regime,  $F_{S1}$  varies little as the pressure is changed from 0.79 to 0.45 MPa. At a superficial gas velocity of approximately 3.4 m/s, Tables 2 and 3 show frequencies of 52 and 50 pulses per minute, Tables 4 and 5 show frequencies of 26 and 24 pulses per minute, and Tables 6 and 7 show frequencies of 14 and 18 pulses per minute.

$F_{S2}$  varies irregularly with gas flow rate in the slug flow regime, but does, generally, mimic the change in  $F_{S1}$ , increasing with an increase in gas flow rate. Table 4 shows that  $F_{S2}$  increases from 20 to 48 pulses per minute as the superficial gas velocity increased from 1.2 to 7.4 m/s. Occasionally,  $F_{S2}$  initially dropped with increasing gas flow rate, indicating the transition from plug flow to slug flow. Table 5 shows that at a superficial liquid velocity of 1.0 m/s,  $F_{S2}$  decreased from 34 to 22 pulses per minute, as the superficial gas velocity was increased from 1.3 to 3.4 m/s.

$F_{S2}$  increased with increasing liquid flow rate in the slug flow regime but varied little with pressure. At approximately 3.4 m/s superficial gas velocity, Tables 2 and 3 show frequencies of 60 and 46 pulses per minute. Tables 4 and 5 show frequencies of 26 and 22 pulses per minute, and Tables 6 and 7 show frequencies of 8 and 10 pulses per minute.

$F_V$  varied similarly to  $F_{S2}$ .  $F_V$  varied irregularly with gas flow rate, decreasing in the transition from plug flow to slug flow and increasing with an increase in gas flow rate in the slug flow regime. Table 5 shows that at a superficial liquid velocity of 1.0 m/s the frequency decreased from 42 to 18 slugs per minute while the superficial gas velocity increased from 1.3 to 3.4 m/s.  $F_V$  then becomes 20 and 54 slugs per minute at 4.9 and 7.8 m/s superficial gas velocity, respectively.  $F_V$  varies erratically with pressure.

As the liquid flow rate increased, in the slug flow regime,  $F_V$  increased. Tables 3, 5, and 7 show that at a superficial gas velocity of approximately 3.4 m/s, the frequency varied from 34 to 18 to 10 slugs per minute at superficial liquid velocities of 1.5, 1.0, and 0.5 m/s, respectively. Tables 2 - 7 also show that the pressure drop increases with gas and liquid flow rates in the slug flow regime but decreases slightly with an increase in pressure.

Tables 9 - 20 present pressure drop and slug frequency data for 80% water cut at 5° inclination and system pressures of 0.27, 0.79, and 1.13 MPa. These tests only utilized one differential pressure tap, but tests 5 and 6 included acoustic signals. Due to the low gas flow rates, the single tap will be sufficient to determine flow type and slug frequency as shown in the method validation. Acoustic frequency and the velocity between acoustic sensors have also been reported.

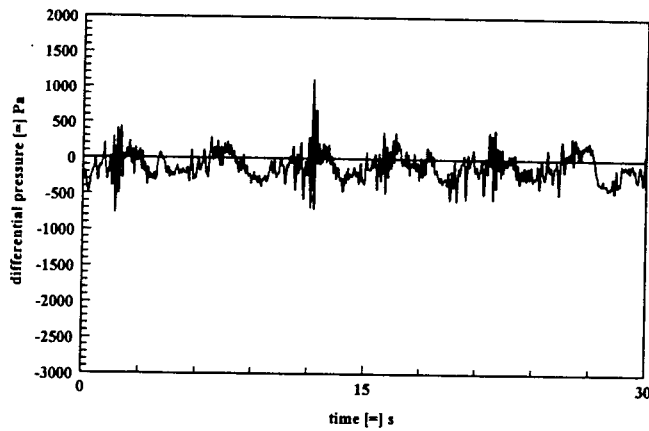


Figure 4: Plug flow sample differential pressure trace at low pressure.

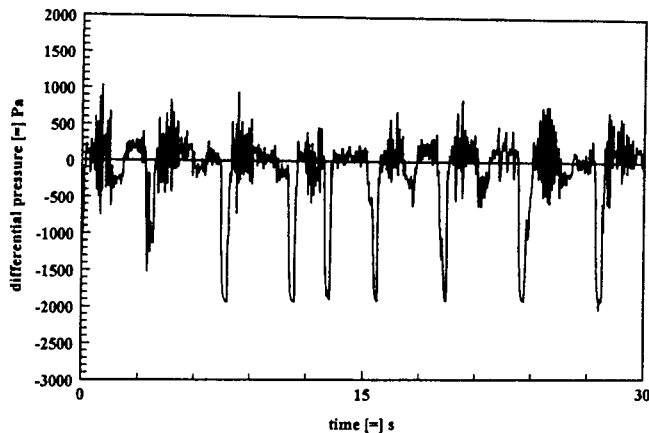


Figure 5: Slug flow sample differential pressure trace at low pressure.

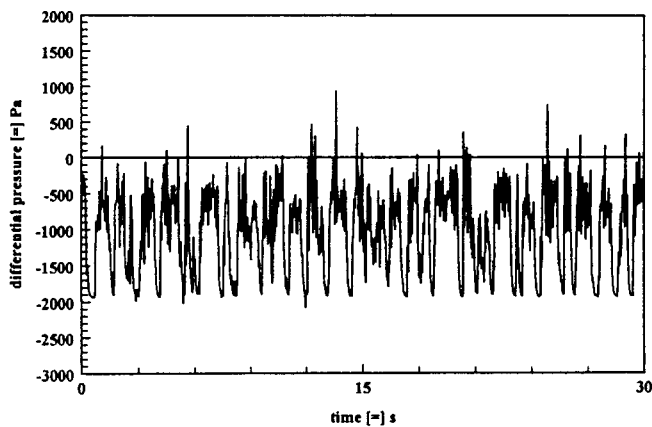


Figure 6: Slug-annular flow sample differential pressure trace at low pressure.

bridge the pipe. The rolling wave velocity was calculated to be 40 - 50% less than the slug front velocity.

Figure 6 is a differential pressure trace for slug-annular flow in the low pressure system. First analysis of this trace falsely predicts 52 slugs per minute. Videotape analysis of this flow showed that it was intermittent in nature with only 23 slugs and pseudo-slugs per minute. The video also recorded additional waves that contributed to the differential pressure fluctuation frequency. An additional review of the videotape demonstrated, again, that the slug velocity was nearly twice that of the rolling wave. Pseudo-slug velocities were typically 10% less than fully developed slugs.

From this comparison, it is clear that two criteria must be met in establishing slug flow. Not only must a minimum differential pressure fluctuation of 1,500 Pa occur, but the front velocity must be appropriate for

that of a slug. Utilizing two transducers, a fixed length apart, allows for this calculation. This characteristic was used in the high-pressure system to identify slugs from the pressure traces of the transducers.

## EXPERIMENTAL SETUP

The high pressure experiments were all performed in an 18-m long, 9.7-cm inner diameter, high pressure (13 MPa), high temperature (90 °C), inclinable flow loop shown in Figure 7. The entire system is manufactured

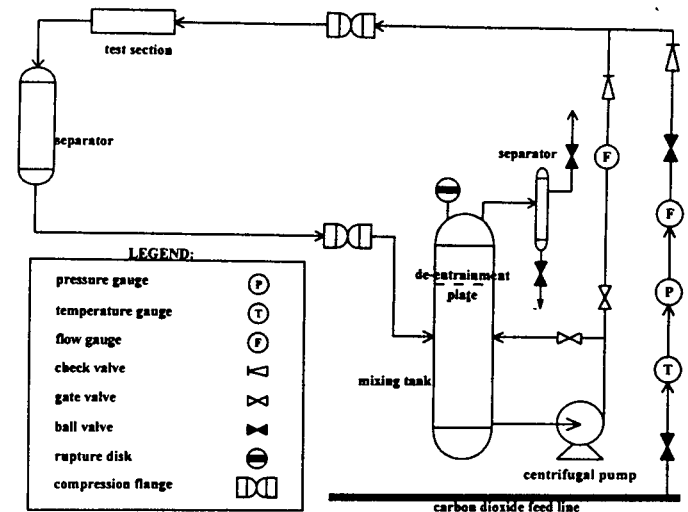


Figure 7: High-pressure, inclinable flow system process flowsheet from 316 stainless steel.

A predetermined oil and water mixture is stored within a 1.4 m<sup>3</sup> mixing tank. The liquid is moved through the system by a 3 - 15 kW variable speed centrifugal pump. The flow is then controlled within a range of zero to 100 m<sup>3</sup>/hr with a combination of the variable speed pump and a recycle stream. The recycle stream also serves to provide agitation in the mixing tank. The flow rate is metered with a frequency analyzer coupled with an in-line turbine.

A 2-MPa feed line supplies carbon dioxide gas from a 20,000 kg receiver. After passing through a pressure regulator, the gas flow rate is metered with a variable area flow meter. The gas then passes through a check valve and into the liquid flow, the combined flow enters the test loop through a compression flange, allowing the inclination to be set at any angle.

Vancko and Jepson (1995) observed that at an inclination of +5°, the slug frequency was 1½ to 2 times greater at a location one meter into inclination, than it was fifteen meters into the inclination. Thus, the test section for this system is located near the end of the 18-m long flow loop and illustrated in Figure 8. Temperature is determined with a type-K

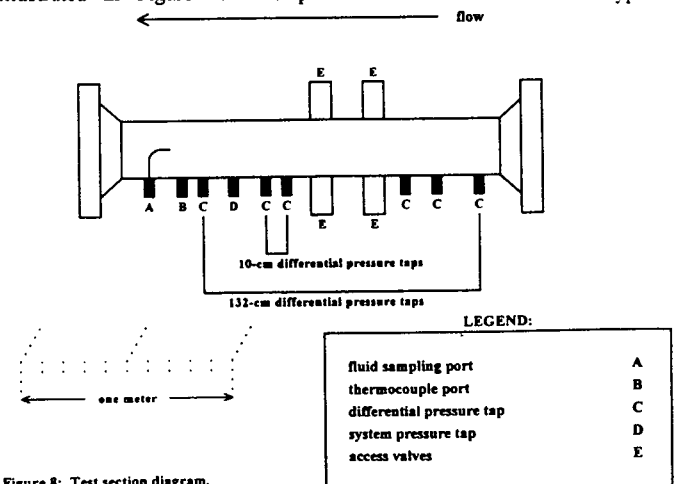


Figure 8: Test section diagram.

$F_{S1}$  varied little with gas flow rate, in the slug flow regime, at these conditions. The frequency did increase with increasing liquid flow rate. At nearly 2.6 m/s superficial gas velocity, Tables 9, 10, 11, and 12 show frequencies of 18, 33, 48, and 66 pulses per minute at superficial liquid velocities of 0.1, 0.5, 1.0, and 1.5 m/s, respectively. Again, the frequency varied little with pressure in the slug flow regime. Acoustic frequencies and velocities are reported for points of reference under varying conditions.

As shown using the non-visual flow determination technique, a differential pressure trace in the form of a low frequency sine wave indicated plug flow. Additionally, a sudden decrease in  $F_{S2}$  and  $F_V$  with a slight increase in gas flow rate indicated plug flow to slug flow transition. Slug flow was declared where the 132-cm differential pressure drop exceeded 1,500 Pa and  $F_V$  matched  $E_2$ . Pseudo-slug flow was marked where the conditions of slug flow were met with the exception of  $F_V$  being approximately 50% that of  $F_{S2}$ . Slug-annular flow was declared where the differential pressure traces were still intermittent, yet  $F_V$  was at or near zero.

Figure 11 is a flow regime map for 100% water cut, 0° inclination, and 0.45 MPa. The transition from stratified to intermittent flow occurs at

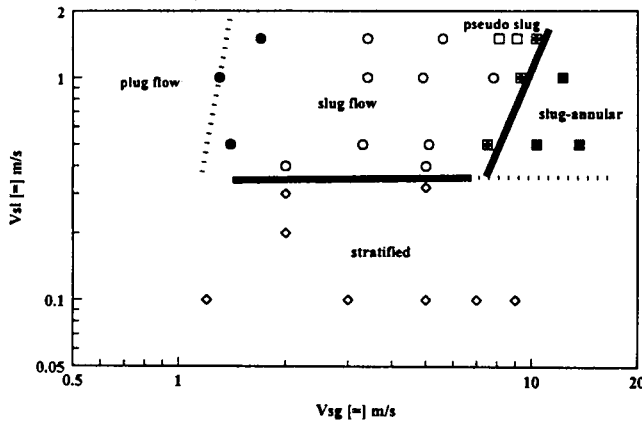


Figure 11: Flow regime map for 100% ASTM seawater, 0° inclination, 0.45 MPa.

approximately 0.35 m/s superficial liquid velocity. The transition from slug flow to slug-annular flow occurred at superficial gas velocities of approximately 7 to 9 m/s, with a pseudo-slug flow pattern occurring above 1.0 m/s superficial liquid velocity. Figure 12 is a flow regime map for 100% water cut, 0° inclination, and 0.79 MPa. From this flow map, the only effect

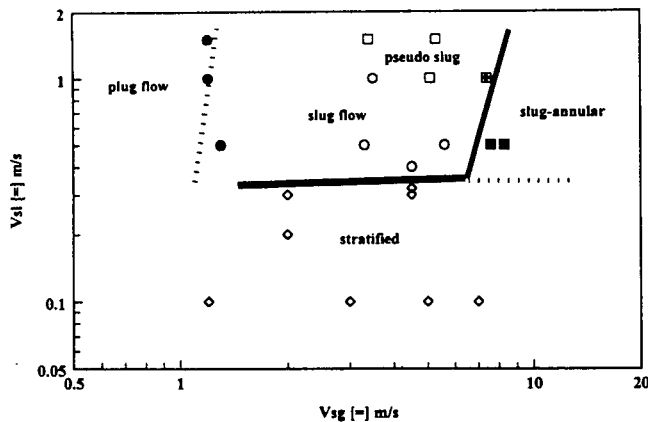


Figure 12: Flow regime map for 100% ASTM seawater, 0° inclination, 0.79 MPa.

of pressure is the increase of the pseudo-slug flow pattern in the slug flow regime. Increasing the pressure from 0.45 to 0.79 MPa forced the pseudo-slug flow pattern to occur at superficial liquid velocities as low as 0.5 m/s, as it begins to dominate the slug flow regime. This was expected as it is the gas-dominated end of the flow pattern map where density-driven effects are more apparent, thus the greater effect of pressure. Figure 13 is a flow regime map for 80% water cut, 5° inclination, and 0.27 MPa. Here, the stratified to intermittent flow transition shifted below a superficial liquid velocity of 0.1 m/s, allowing slug flow to dominate the range of normal operating conditions.

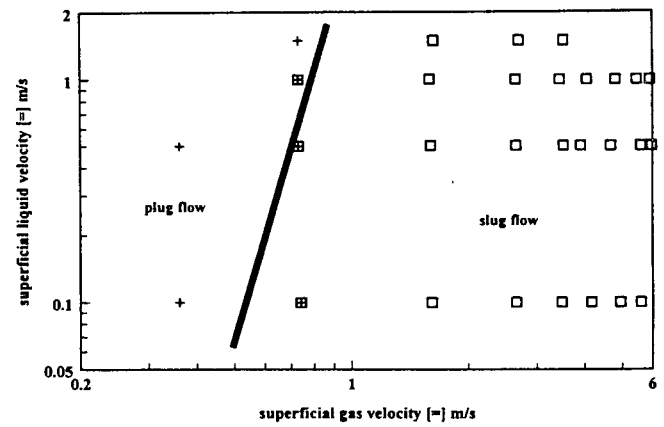


Figure 13: Flow regime map for 80% water cut, inclined 5°, 0.27 MPa.

Figure 14 represents the flow pattern data for 80% water cut, +5° inclination, and system pressures of 0.27, 0.79, and 1.13 MPa. Filled data

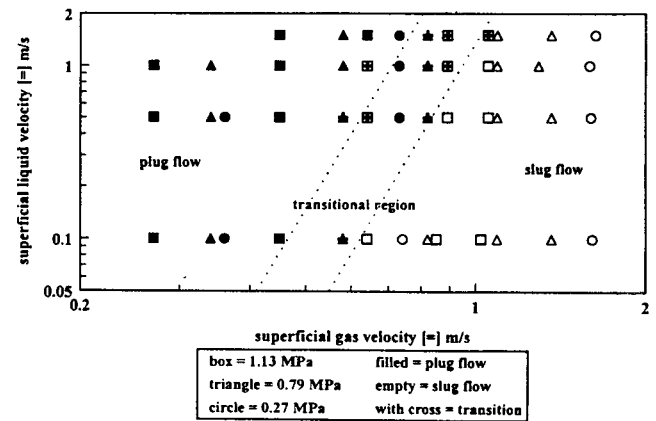


Figure 14: Flow type scatter plot for 80% water cut, inclined +5°.

points represent plug flow, while empty data points represent slug flow. Data points with a cross mark locations where the flow illustrated properties of both plug and slug flow. The plug flow to slug flow transition has been located by noting where a variation in the superficial gas velocity, of 0.1 m/s, will shift into definite plug or slug flow regimes. It can be seen in this Figure that the transition is invariant with pressure in the range tested. These Figures also show that slug flow truly occurs at 0.1 m/s superficial liquid velocity in inclined flow at all pressures tested.

## CONCLUSIONS

The following conclusions may be drawn:

- At high gas flow rates, non-visual determination of slug flow by pressure fluctuation measurements must be coordinated with slug front velocity information.
- At high gas flow rates, non-visual determination of slug frequency by pressure fluctuation measurements must be coordinated with slug front velocity measurements to verify that the pulses are slugs.

Additionally, for the conditions studied:

- The slug frequency increased with increasing liquid flow rate, regardless of liquid composition, inclination, and pressure.
- The slug frequency was not variant with pressure.
- Increasing the pressure has no effect upon the stratified/intermittent boundary.

- Increasing the pressure has no effect upon the plug flow/slugg flow transition.
- Increasing the pressure causes pseudo-slugg flow to dominate the slug flow regime.
- Increasing the inclination forces the stratified/intermittent boundary to occur at lower liquid flow rates.

#### RECOMMENDATIONS

It is recommended that the influence of pressure be investigated for higher pressures, and the inclination should be increased to +45° and ultimately to +90°. At selected inclinations and pressures, the water cut should be further varied to verify its effects.

Using this data, a more comprehensive mathematical model of flow type should be developed to include effects of pressure, inclination, and additional phases. Likewise, models of slug properties should be created based upon physical criteria. The method developed here needs to be utilized in the field at operating conditions, to verify its use and then to obtain operational data for mathematical model validation. These models will then be applicable to determine appropriate flow information for analyzing corrosion mechanisms.

#### ACKNOWLEDGMENTS

This work has been sponsored by the NSF I/UCRC Corrosion in Multiphase Systems Center. Additional thanks to Jeff Maley for experimental assistance and to Dr. Tony Green for editorial comments.

#### REFERENCES

- Barnea, D., O. Shoham, Y. Taitel, and A.E. Dukler, "Flow Pattern Transitions for Gas-Liquid Flow in Horizontal and Inclined Pipes; Comparison of Experimental Data with Theory", *Int. J. Multiphase Flow*, **6**, 217-225, 1980.
- Barnea, D., O. Shoham, Y. Taitel, and A.E. Dukler, "Gas Liquid in Inclined Tubes: Flow Pattern Transitions for Upward Flow", *Chem. Engng. Sci.*, **40**, 131-136, 1985.
- Dukler, A. E. and M. G. Hubbard, "A Model for Gas-Liquid Flow in Horizontal or Near Horizontal Tubes", *Ind. Eng. Chem. Fund.*, **14**, 337-347, 1975.
- Fan, Z., Z. Ruder, and T. J. Hanratty, "Pressure Profiles for Slugs in Horizontal Pipelines", *Int. J. Multiphase Flow*, **19**, 1993.
- Gould, T. L., M. Tek, and D. L. Katz, "Two Phase Flow Through Vertical, Inclined or Curved Pipes", *J. Petrol. Tech.*, **26**, 915-926, 1974.
- Gopal, M., "Visualization and Mathematical Modeling of Multiphase Horizontal Slug Flow", Ph.D. Thesis, Ohio University, Athens, Ohio, 1994.
- Govier, Aziz, and Fogarasi, *J. Can. Petrol. Tech.*, **11**, 38+, 1972.
- Gregory, G. A. and D. S. Scott, "Correlation of Liquid Slug Velocity and Frequency in Horizontal Cocurrent Gas Liquid Flow", *AIChE J.*, **15**, 933-935, 1969.
- Jepson, W. P., "Modeling the Transition to Slug Flow in Horizontal Conduit", *Can. J. Chem. Engng.*, **67**, 731-740, 1989.
- Jepson, W. P. and R. E. Taylor, "Slug Flow and Its Transition in Large Diameter Horizontal Pipes", *Int. J. Multiphase Flow*, **19**, 411-420, 1993.
- Kaul, Ashwini, "Study of Slug Flow Characteristics and Performance of Corrosion Inhibitors, in Multiphase Flow, in Horizontal Oil and Gas Pipelines", M.S. Thesis, Ohio University, Athens, Ohio, 1995.
- Kokal, S. L. and J. F. Stanislav, "An Experimental Study of Two Phase Flow in Inclined Pipes", personal communication with W. P. Jepson, 1986.
- Kouba, G. E. and W. P. Jepson, "The Flow of Slugs in Horizontal, Two Phase Pipelines", Pipeline Engineering Symposium, American Society of Mechanical Engineers, 1989.
- Lee, Asi Hsin, "A Study of Flow Regime Transition for Oil-Water-Gas Mixtures in Large-Diameter Horizontal Pipelines", M.S. Thesis, Ohio University, Athens, Ohio 1993.
- Lin, P. Y. and T. J. Hanratty, "Detection of Slug Flow from Pressure Measurements", *Int. J. Multiphase Flow*, **13**, 549-563, 1987.
- Mandhane, J. M., G. A. Gregory, and K. Aziz, "A Flow Pattern Map for Gas-Liquid Flow in Horizontal Pipes", *Int. J. Multiphase Flow*, **1**, 537-553, 1974.
- Nicholson, M. K., K. Aziz, and G. A. Gregory, "Intermittent Two Phase Flow in Horizontal Pipes: Predictive Models", *Can. J. Chem. Engng.*, **56**, 653-663, 1978.
- Spedding, P. L. and D. R. Spence, "Flow Regimes in Two-Phase Gas-Liquid Flow", *Int. J. Multiphase Flow*, **19**, 245-280, 1993.
- Stanislav, J. F., S. Kokal, and M. K. Nicholson, "Intermittent Gas-Liquid Flow in Upward Inclined Pipes", *Int. J. Multiphase Flow*, **12**, 325-335, 1986.
- Taitel, Y. and A. E. Dukler, "A Model for Predicting Flow Regime Transitions in Horizontal and Near Horizontal Gas-Liquid Flow", *AIChE J.*, **22**, 47-55, 1976.
- Vancko, R. M., Jr. and W. P. Jepson, "Multiphase Flow Mechanisms in 5° Inclined Pipes", video produced by NSF I/UCRC Corrosion in Multiphase Systems Center, 1995.

#### APPENDIX

Table 1: Test matrix.

	angle (°)	water cut (%)	pressure (MPa)	V <sub>sl</sub> (m/s)	V <sub>sg</sub> (m/s)	132-cm taps	10-cm taps	other
1	0	45	0.14	0.1-1.5	0-11	X	---	videotape
2	0	100	0.45	0.1-1.5	0-11	X	X	---
3	0	100	0.79	0.1-1.5	0-7	X	X	---
4	5	80	0.27	0.1-1.5	0-6	X	---	---
5	5	80	0.79	0.1-1.5	0-1.5	X	---	acoustic
6	5	80	1.13	0.1-1.5	0-1	X	---	acoustic

Table 2: Flow characteristic summary for 100% water cut at 0° inclination,  $V_{sl} = 1.5$  m/s, 0.79 MPa.

$V_{wg}$ [=] m/s	$V_l$ [=] m/s	$F_{s1}$ [=] pulse/min	$F_{s2}$ [=] pulse/min	$F_v$ [=] slugs/min	Pressure Drop [=] Pa
1.2	3.2	34 ± 4	26 ± 4	26 ± 4	1100 ± 100
3.4	5.9	52 ± 4	20 ± 4	14 ± 4	2200 ± 400
5.3	8.2	78 ± 4	14 ± 4	16 ± 4	3000 ± 500

Table 3: Flow characteristic summary for 100% water cut at 0° inclination,  $V_{sl} = 1.5$  m/s, 0.45 MPa.

$V_{wg}$ [=] m/s	$V_l$ [=] m/s	$F_{s1}$ [=] pulse/min	$F_{s2}$ [=] pulse/min	$F_v$ [=] slugs/min	Pressure Drop [=] Pa
1.7	3.8	50 ± 4	37 ± 4	31 ± 4	1200 ± 200
3.4	5.9	50 ± 4	22 ± 4	17 ± 4	2300 ± 400
5.6	8.5	68 ± 4	22 ± 4	26 ± 4	3700 ± 700
8.1	11.5	94 ± 4	25 ± 4	20 ± 4	4300 ± 800
9.1	12.7	98 ± 4	29 ± 4	14 ± 4	4000 ± 600
10.3	14.2	110 ± 4	16 ± 4	9 ± 4	4500 ± 800

Table 4: Flow characteristic summary for 100% water cut at 0° inclination,  $V_{sl} = 1.0$  m/s, 0.79 MPa.

$V_{wg}$ [=] m/s	$V_l$ [=] m/s	$F_{s1}$ [=] pulse/min	$F_{s2}$ [=] pulse/min	$F_v$ [=] slugs/min	Pressure Drop [=] Pa
1.2	2.6	20 ± 4	29 ± 4	22 ± 4	600 ± 100
3.5	5.4	26 ± 4	11 ± 4	7 ± 4	1500 ± 300
5.1	7.3	30 ± 4	15 ± 4	6 ± 4	2200 ± 300
7.4	10.1	50 ± 4	18 ± 4	5 ± 4	2300 ± 400

Table 5: Flow characteristic summary for 100% water cut at 0° inclination,  $V_{sl} = 1.0$  m/s, 0.45 MPa.

$V_{wg}$ [=] m/s	$V_l$ [=] m/s	$F_{s1}$ [=] pulse/min	$F_{s2}$ [=] pulse/min	$F_v$ [=] slugs/min	Pressure Drop [=] Pa
1.3	2.8	42 ± 4	29 ± 4	22 ± 4	1100 ± 200
3.4	5.3	24 ± 4	11 ± 4	9 ± 4	2600 ± 600
4.9	7.1	30 ± 4	13 ± 4	11 ± 4	2900 ± 600
7.8	10.6	80 ± 4	27 ± 4	29 ± 4	3900 ± 700
9.3	12.4	76 ± 4	27 ± 4	9 ± 4	3900 ± 800
12.2	15.8	80 ± 4	20 ± 4	0 ± 4	3900 ± 800

Table 6: Flow characteristic summary for 100% water cut at 0° inclination,  $V_{sl} = 0.5$  m/s, 0.79 MPa.

$V_{wg}$ [=] m/s	$V_l$ [=] m/s	$F_{s1}$ [=] pulse/min	$F_{s2}$ [=] pulse/min	$F_v$ [=] slugs/min	Pressure Drop [=] Pa
1.3	2.2	14 ± 4	17 ± 4	8 ± 4	800 ± 400
3.3	4.6	14 ± 4	12 ± 4	4 ± 4	900 ± 200
5.6	7.3	6 ± 4	11 ± 4	3 ± 4	400 ± 200
7.6	9.7	12 ± 4	19 ± 4	1 ± 4	700 ± 300
8.3	10.6	20 ± 4	22 ± 4	0 ± 4	900 ± 500

Table 7: Flow characteristic summary for 100% water cut at 0° inclination,  $V_{sl} = 0.5$  m/s, 0.45 MPa.

$V_{wg}$ [=] m/s	$V_l$ [=] m/s	$F_{s1}$ [=] pulse/min	$F_{s2}$ [=] pulse/min	$F_v$ [=] slugs/min	Pressure Drop [=] Pa
1.4	2.3	22 ± 4	11 ± 4	8 ± 4	1200 ± 100
3.3	4.6	18 ± 4	14 ± 4	5 ± 4	1100 ± 200
5.1	6.7	26 ± 4	13 ± 4	4 ± 4	1600 ± 200
7.5	9.6	26 ± 4	13 ± 4	3 ± 4	2000 ± 600
10.3	13.0	42 ± 4	19 ± 4	2 ± 4	2000 ± 700
13.6	16.9	60 ± 4	7 ± 4	0 ± 4	2200 ± 400

Table 8: Flow characteristic summary for 100% water cut at 0° inclination,  $V_{sl} = 0.1$  m/s, 0.45 MPa and 0.79 MPa.

No slug flow results were seen at either pressure for a  $V_{sl} = 0.1$  m/s. All of the flow encountered was stratified flow.

Table 9: Flow characteristic summary for 80% water cut at 5° inclination,  $V_{sl} = 0.1$  m/s, 0.27 MPa.

$V_{wg}$ [=] m/s	$V_l$ [=] m/s	$F_{s1}$ [=] pulse/min	Pressure Drop [=] Pa
1.6	1.9	21 ± 4	3200 ± 600
2.6	3.2	18 ± 4	3400 ± 800
3.5	4.3	16 ± 4	3400 ± 600
4.1	5.0	15 ± 4	2800 ± 600
4.9	6.0	15 ± 4	2200 ± 500
5.5	6.7	12 ± 4	2000 ± 500
6.0	7.3	12 ± 4	1800 ± 300

Table 10: Flow characteristic summary for 80% water cut at 5° inclination,  $V_{sl} = 0.5$  m/s, 0.27 MPa.

$V_w$ [=] m/s	$V_t$ [=] m/s	$F_{s1}$ [=] pulse/min	Pressure Drop [=] Pa
1.6	2.5	33 ± 4	3600 ± 800
2.6	3.7	33 ± 4	3800 ± 800
3.5	4.8	33 ± 4	3800 ± 800
3.9	5.3	33 ± 4	3800 ± 600
4.6	6.1	33 ± 4	3900 ± 300
5.4	7.1	33 ± 4	4200 ± 300
5.9	7.7	39 ± 4	4100 ± 300

Table 11: Flow characteristic summary for 80% water cut at 5° inclination,  $V_{sl} = 1.0$  m/s, 0.27 MPa.

$V_w$ [=] m/s	$V_t$ [=] m/s	$F_{s1}$ [=] pulse/min	Pressure Drop [=] Pa
1.6	3.1	42 ± 4	3500 ± 500
2.6	4.3	48 ± 4	4200 ± 400
3.4	5.3	51 ± 4	4400 ± 300
4.0	6.0	42 ± 4	4400 ± 600
4.8	7.0	42 ± 4	4400 ± 600
5.4	7.7	42 ± 4	4400 ± 600
5.8	8.2	45 ± 4	4200 ± 600

Table 12: Flow characteristic summary for 80% water cut at 5° inclination,  $V_{sl} = 1.5$  m/s, 0.27 MPa.

$V_w$ [=] m/s	$V_t$ [=] m/s	$F_{s1}$ [=] pulse/min	Pressure Drop [=] Pa
1.6	3.7	78 ± 4	3200 ± 600
2.7	5.0	66 ± 4	4600 ± 600
3.5	6.0	60 ± 4	4600 ± 600

Table 13: Flow characteristic summary for 80% water cut at 5° inclination,  $V_{sl} = 0.1$  m/s, 0.79 MPa.

$V_w$ [=] m/s	$V_t$ [=] m/s	$F_{s1}$ [=] pulse/min	Acoustic Frequency [=] pulse/min	$V_t$ Acoustic [=] m/s	Pressure Drop [=] Pa
0.3	---	-----	20 ± 0.7	-----	-----
0.8	1.1	24 ± 4	-----	-----	2800 ± 300
1.1	1.4	21 ± 4	-----	3.0 ± 0.3	3100 ± 700
1.4	1.8	19 ± 4	-----	-----	3500 ± 700

Table 14: Flow characteristic summary for 80% water cut at 5° inclination,  $V_{sl} = 0.5$  m/s, 0.79 MPa.

$V_w$ [=] m/s	$V_t$ [=] m/s	$F_{s1}$ [=] pulse/min	Acoustic Frequency [=] pulse/min	$V_t$ Acoustic [=] m/s	Pressure Drop [=] Pa
1.1	1.9	34 ± 4	-----	-----	3100 ± 900
1.4	2.3	34 ± 4	-----	-----	3100 ± 700

Table 15: Flow characteristic summary for 80% water cut at 5° inclination,  $V_{sl} = 1.0$  m/s, 0.79 MPa.

$V_w$ [=] m/s	$V_t$ [=] m/s	$F_{s1}$ [=] pulse/min	Acoustic Frequency [=] pulse/min	$V_t$ Acoustic [=] m/s	Pressure Drop [=] Pa
0.8	2.2	-----	-----	2.6 ± 0.2	-----
1.1	2.5	60 ± 4	185 ± 11	4.4 ± 0.3	3100 ± 300
1.3	2.8	60 ± 4	-----	-----	3100 ± 300

Table 16: Flow characteristic summary for 80% water cut at 5° inclination,  $V_{sl} = 1.5$  m/s, 0.79 MPa.

$V_w$ [=] m/s	$V_t$ [=] m/s	$F_{s1}$ [=] pulse/min	Acoustic Frequency [=] pulse/min	$V_t$ Acoustic [=] m/s	Pressure Drop [=] Pa
1.1	3.1	-----	-----	4.1 ± 0.3	-----
1.4	3.5	76 ± 4	-----	-----	2400 ± 600

Table 17: Flow characteristic summary for 80% water cut at 5° inclination,  $V_{sl} = 0.1$  m/s, 1.13 MPa.

$V_w$ [=] m/s	$V_t$ [=] m/s	$F_{s1}$ [=] pulse/min	Acoustic Frequency [=] pulse/min	$V_t$ Acoustic [=] m/s	Pressure Drop [=] Pa
0.6	0.8	26 ± 4	-----	-----	2200 ± 300
0.8	1.1	22 ± 4	-----	-----	2800 ± 300
1.0	1.3	22 ± 4	-----	-----	2800 ± 700

Table 18: Flow characteristic summary for 80% water cut at 5° inclination,  $V_{sl} = 0.5$  m/s, 1.13 MPa.

$V_w$ [=] m/s	$V_t$ [=] m/s	$F_{s1}$ [=] pulse/min	Acoustic Frequency [=] pulse/min	$V_t$ Acoustic [=] m/s	Pressure Drop [=] Pa
0.1	0.7	-----	30 ± 1.5	1.1 ± 0.1	-----
0.3	1.0	-----	32 ± 1.7	2.4 ± 0.4	-----
0.5	1.2	-----	48 ± 3.8	2.4 ± 0.4	-----
0.7	1.4	-----	52 ± 4.5	1.6 ± 0.2	-----
0.9	1.7	40 ± 4	40 ± 2.7	2.8 ± 0.6	2800 ± 900
1.1	1.9	40 ± 4	48 ± 3.8	2.8 ± 0.6	2600 ± 700